

LOSS OF DUCTILITY AND STRENGTH OF REINFORCING STEEL DUE TO PITTING CORROSION

R. HINGORANI^{*}, F. PÉREZ[†], J. SÁNCHEZ[†], J. FULLEA^{*}, C. ANDRADE^{*}, P. TANNER[†]

^{*} Centro de Seguridad y Durabilidad Estructural y de Materiales (CISDEM-CSIC-UPM).
C/ Serrano Galvache, 4 - 28033 Madrid, Spain
e-mail: hingorani@ietcc.csic.es, fullea@ietcc.csic.es, andrade@ietcc.csic.es

[†] Instituto de Ciencias de la Construcción Eduardo Torroja (IETcc-CSIC).
C/ Serrano Galvache, 4 - 28033 Madrid, Spain
e-mail: ferlingote@gmail.com, javier.sanchez@csic.es, tannerp@ietcc.csic.es

Key words: Reinforcing steel, pitting corrosion, mechanical properties, ductility, numerical study

Abstract: Any number of studies have been conducted in the past to analyse mechanical behaviour of corroded reinforcement steel bars. The general procedure adopted in most studies is threefold: In a first step, rebars are subjected to an accelerated corrosion procedure. Then the corrosion degree, which expresses the material loss of the specimen due to corrosion, is determined. Finally, the rebars are subjected to tensile testing and the obtained mechanical properties are related to the corrosion degree.

However, further research is certainly needed on the consequences of localized corrosion phenomena. In presence of chloride anions able to break the passive layer, corrosion pits may be generated on the steel reinforcement. In this case, loss of mechanical properties will depend primarily on localized corrosion related aspects, like geometry and distribution of the pits, rather than on general material loss of the bars. This calls for an explicit geometrical characterization of pitting corrosion and analysis of its consequences on mechanical performance.

In the present work, a numerical analysis on the tensile behaviour of B500B rebars, affected by an elliptically shaped corrosion pit, has been carried out. In a parametrical study, the principal mechanical properties characterizing strength and ductility of the bars have been determined as a function of the pit dimensions. Beside the maximum pit depth, the slenderness of the pits (length to depth ratio) has been found to affect considerably the mechanical properties of the rebars. The ductility of the bars is particularly sensitive to changes in pit geometry.

1 INTRODUCTION

Several experimental studies have been carried out in the past with the aim to assess the mechanical properties of corrosion affected reinforcing steel bars [1-9]. In most of those studies, test specimens are exposed to a certain type of corrosion process, followed by their mechanical characterization by means of tensile testing. The obtained mechanical

properties from the tests are normally related to corrosion degree Q_{corr} , which indicates the percentage loss of material due to the corrosion process. In view of the assessment of mechanical performance of corrosion-affected reinforced concrete structures, establishing such relations seems to be generally useful since Q_{corr} can be easily estimated from corrosion rate measurements [10].

However, the estimation of mechanical properties from Q_{corr} is subjected to considerable uncertainties, especially when rebars are affected by local corrosion attack. The experimental results obtained in several studies evidence that certain mechanical parameters, like for instance the ultimate deformation, may be very sensitive to the effects introduced by corrosion pits [3-8]. Care should therefore be taken, where corrosion attack is governed by the presence of chloride ions, for instance. In that case, the mechanical parameters obtained from models depending on Q_{corr} , should be interpreted as a rough estimates only, and even run the risk of being overestimated.

This calls for a complementary, explicit analysis of localized corrosion effects. For instance, models should be available from which a description of localized corrosion characteristics, like pit geometry and distribution, may be drawn. Moreover, models for a closer estimation of mechanical properties as a function of such characteristics are required, subject addressed in the present paper. To be accurate, a numerical study has been carried out with the aim to analyze the influence of geometrical characteristics of corrosion pits on the mechanical properties of a reinforcing steel bar.

Section 2 of the present contribution contains a summary of a previous literature review on the mechanical properties of reinforcing steel bars affected by corrosion. In section 3, the approach and the main results of the numerical study performed are presented. The paper ends with concluding remarks in section 4.

2 MECHANICAL PROPERTIES OF CORRODED REBARS

Several studies dedicated to the analysis of mechanical properties of corroded rebars have been reviewed. With the exception of [1], where specimens extracted from a concrete bridge have been analyzed, the determination of mechanical properties of corroded rebars is based on an experimental procedure which is characterized by three fundamental steps:

In a first step the reinforcing steel bars, contained in solution, embedded in concrete specimens or exposed to salt spray [2], are subjected to an accelerated corrosion process with applied current densities varying from 10 to 2000 $\mu\text{A}/\text{cm}^2$. Secondly, the corroded specimens are geometrically characterized. This is generally done by weighing the amount of material lost during the corrosion process. From this data, the corrosion degree Q_{corr} is obtained and the corresponding remaining average cross-sectional area $A_{s,corr,av}$ of the corroded specimen is determined from (1), where A_{s0} is the cross-sectional area of the non-corroded rebar.

$$A_{s,corr,av} = (1 - Q_{corr} / 100)^{0.5} \cdot A_{s0} \quad (1)$$

Normally, no explicit geometrical characterization of localized corrosion damage phenomena is being carried out. An exception is given for example in [1,5] where the relationship between the maximum and average depth of corrosion attack is being established, known as the pitting factor according to its definition in the manual Contecvet [10].

The 3-step experimental procedure concludes by subjecting the rebars to tensile tests, recording force and displacement to then obtain the stress-strain curve. Finally, from this curve, the main mechanical properties of the corroded bars are deduced, like yield and tensile strength, and parameters characterizing ductility, as for instance ultimate strain.

In most of the studies [2-8] analyzed, strength of the corroded bars is represented by the ratio of the force applied to the bar, F , to its average remaining cross-sectional area, $A_{s,corr,av}$, obtained from (1). This ratio represents an average stress level in the corroded bar, which in the following will be denominated $\sigma_{corr,av}$.

$$\sigma_{corr,av} = F / A_{s,corr,av} \quad (2)$$

The average stresses corresponding to the yield strength of the bars, $\sigma_{y,corr,av} = F_y / A_{s,corr,av}$, and to its tensile strength, $\sigma_{u,corr,av} = F_u / A_{s,corr,av}$, are of special interest in the context of structural safety assessment. Figure 1 represents the ratios of $\sigma_{y,corr,av}$ and $\sigma_{u,corr,av}$

to the respective resistances of sound bars, σ_{y0} and σ_{u0} , obtained in [5]. The ratios are expressed as a function of corrosion degree Q_{corr} and corresponding linear regression models have been deduced. Such models may then be employed to estimate decrease in yield and ultimate force of corroded rebars. For instance, according to the model deduced by Du et al. [5] represented in Figure 1, a corrosion degree of 20% entails ratios $\sigma_{corr,av} / \sigma_0$ of about 0.90. Applying equations (1) and (2), it may then be concluded that the corresponding yield and ultimate force of corroded rebars are expected to decrease about 20% with respect to the values of sound bars, F_{y0} and F_{u0} . Other experimental studies, for instance [3,4] confirm this rather moderate decrease in load carrying capacity of corroded reinforcement bars.

Another interesting finding from Figure 1 [5] is the tendency of $\sigma_{y,corr,av}$ and $\sigma_{u,corr,av}$ to decrease with increasing Q_{corr} , as well observed in other experimental studies [2-6]. According to Du et al. [5], this shows the increasing influence of corrosion pits on the reinforcement surface and the corresponding stress concentrations which may arise at those pits. Almussalam [8] as well relates significant pit formation to high corrosion degrees.

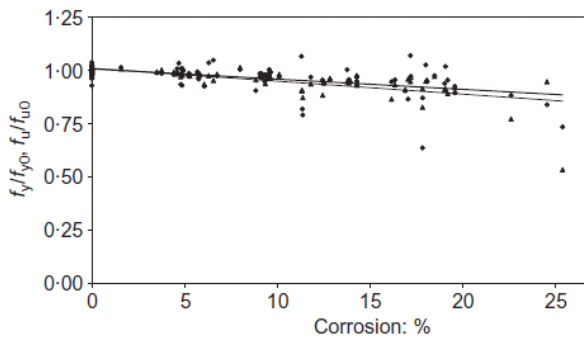


Figure 1: Ratios $\sigma_{y,corr,av} / \sigma_{y0}$ y $\sigma_{u,corr,av} / \sigma_{u0}$ corresponding to 8, 16 and 32mm plain and ribbed bars, as a function of corrosion degree, Q_{corr} [5]

It is important to point out that regression models, like those represented in Figure 1, should be applied with care in case localized corrosion effects are present. Though such effects are implicitly accounted for in this type of models, they run the risk of leading to

inconsistent and even non conservative predictions of load carrying capacity of rebars with significant, irregular corrosion attack. In those cases, the estimation of residual resistance should be completed by use of models which explicitly take account of effects introduced by localized corrosion phenomena, like pits. With this aim, Stewart [11] combines the regression model derived in [5] to estimate ratio $\sigma_{y,corr,av} / \sigma_{y0}$ (Figure 1), with the aforementioned pitting factor in order to perform a reliability analysis of pitting corrosion affected reinforced concrete beams.

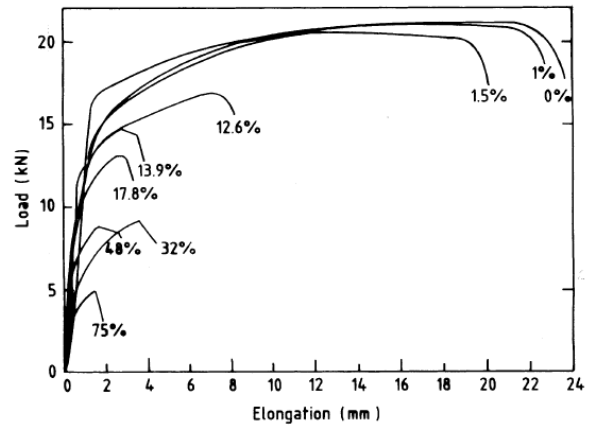


Figure 2: Load-displacement curves corresponding to 6mm bars affected by different Q_{corr} [8]

Another conclusion which may be drawn from the literature review is that corrosion can have a significant impact on the ductility of rebars. In some of the analyzed studies [6,8,9] it is shown that corroded bars may be affected by a very significant reduction of ultimate strain, $\epsilon_{u,corr}$, even in case of moderate Q_{corr} . In Figure 2, taken from the work of Almussalam [8], it is observed that a Q_{corr} of only 12.6% entails a brittle behavior with a reduction of $\epsilon_{u,corr}$ around 65%. However, other authors do not detect such drastic diminishments. Garcia [3,4], for instance, found a reduction in ductility of about 20% when $Q_{corr} \approx 10\%$. The regression models shown in Figure 3, extracted from an experimental study on ductility of corroded rebars [6], show up a reduction of $\epsilon_{u,corr}$ around 40-55%, when corrosion degree is 15%. Moreover it may be seen in Figure 3 that ultimate strain decreases clearly with increasing Q_{corr} , what could equally be observed in other studies [1,3,4,7-

9]. As formerly reported in the context of load carrying capacity of corroded rebars, this could be indicative of the rising influence of localized corrosion effects with increasing corrosion degree. It should also be remembered that regression models like the one shown in Figure 3, depending on Q_{corr} only, should be carefully employed when bars suffer from an irregular corrosion attack. The above reported, widely scattered experimental results from [1,3,4,6-9] suggest that ultimate strain of rebars is highly sensitive to pitting corrosion. In the reviewed literature, there is a general agreement that brittle behavior of corroded rebars may be mainly attributed to the geometrical influences of corrosion pits on the rebar surface and the corresponding strain concentrations at such pits. In [9] a theoretical exercise is carried out to show that ductility of corroded rebars is function of both, the non-uniform distribution of corrosion pits along the bar length and the local penetration depths. However, no models were found within the here reported literature which would allow for a more detailed explanation of ductility decrease as a function of corrosion pit geometry and distribution on the rebars.

Another parameter which characterizes the ductility of a reinforcing steel bar is the ratio of tensile strength to yield strength of the bars. In [1,6,9], where the ratio between the average stresses $\sigma_{u,corr,av}$ and $\sigma_{y,corr,av}$ was experimentally deduced, it is shown that this ratio is not sensitive to variations of Q_{corr} .

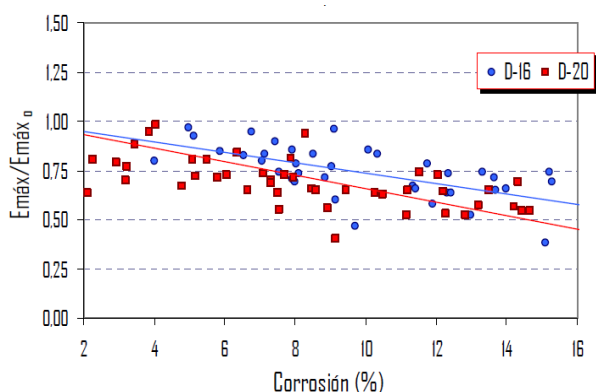


Figure 3: Ratio $\varepsilon_{u,corr}/\varepsilon_{u0}$ as a function of corrosion degree, Q_{corr} , for rebars of 16 and 20 mm diameter [6]

It should also be noted that the

bibliographic review could not clarify whether the reduction of the load bearing capacity and ductility of corroded bars is due exclusively to geometrical effects, like reduction of cross-sectional area and the effects derived from localized corrosion pits. Additionally, it could be possible that the proper mechanical material properties are altered by the corrosion procedure. This would require specific tensile tests on previously corroded, machined rebars, to fully exclude the geometrical effects introduced by corrosion pits.

To summarize the most relevant of the above, localized corrosion may have important effects on the mechanical performance of reinforcing steel bars, especially on its ductility. However, in most of the analyzed studies, the experimentally deduced mechanical parameters of corroded bars are related to corrosion degree only, what could entail inconsistent and even unsafe predictions when significant corrosion pits are present. In that case, a complementary, explicit analysis of localized corrosion effects would be of advantage. Such an explicit analysis requires, amongst others, models which relate the mechanical properties with the geometrical changes induced by localized corrosion in the bars. This subject is being addressed in the present paper. Strictly speaking, a numerical study has been performed, which will be presented in the next section. The objective was to study the mechanical behavior of a reinforcing steel bar depending on the geometrical characteristics of corrosion pits. It should be noted that Cordero [12] performed a similar study which, unlike the present, focused on prestressing steel wires.

3 NUMERICAL STUDY

3.1 Geometry

The numerical study has been carried out with the finite element software COMSOL Multiphysics. A 3-dimensional model has been developed by intercepting a rebar of diameter d with an ellipsoid characterized by its semi-axis a , b and p , defining in that way an elliptically shaped corrosion pit. This is shown

schematically in Figure 4.

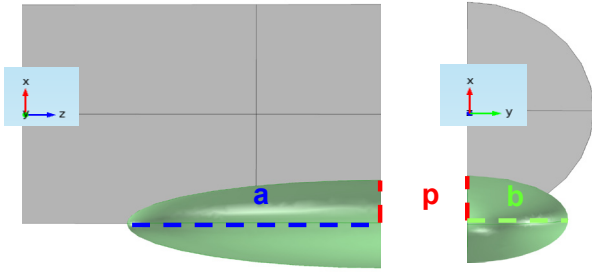


Figure 4: Modeling of a notched bar by interception of a cylinder with an ellipsoid of semi-axis a , b and p

Moreover, from Figure 4 it can be observed that the bar symmetry in both longitudinal (with respect to the x - y plane) and transverse direction (with respect to the x - z) has been accounted for in the modeling procedure. Considering those two symmetry planes, signalized as well in Figure 5 in blue color, allows for a significant reduction of element numbers and thereby for a more efficient computational procedure.

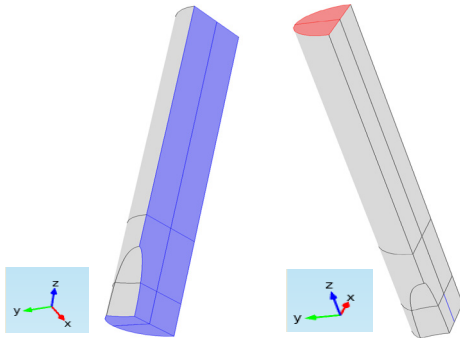


Figure 5: Symmetry planes and tensile-loading plane at the bar end

In order to cover a large number of cases encountered in practice, the main parameters describing the geometry of both the rebar and the corrosion pit have been varied within reasonable limits yielding a total of 36 cases. The covered parameter ranges are listed below.

- Bar diameter: $d = 12$ and 32 mm
- Relative maximum pit depth: $p/d = 0.05; 0.1; 0.2; 0.4$
- Pit length to depth ratio: $a/p = 1; 5; 10$
- Pit width to depth ratio: $b/p = 1; 2$

(study of cases $b/p = 2$ was limited to bars with $d = 12$ mm)

3.2 Loading

The modeled rebars have been subjected to a progressively incrementing tensile load, applied perpendicular to the red colored plane (Figure 5) at the bar end. Load has been incremented in steps of $F_{u0} \cdot 10^{-2}$, where F_{u0} is the load corresponding to the tensile strength of the sound bars, $F_{u0} = f_{u0} \cdot A_{s0}$. In order to assure that the stress state at the extreme of the bars, where the load was introduced, would not be influenced by the pit, a bar length of $l = 5 \cdot d$ had to be provided. Only the cases characterized by combination of $p/d = 0.4$ and $a/p = 10$, required an increased bar length of $l = 7.5 \cdot d$.

3.3 Mesh characteristics

The number of tetrahedral elements which composed the finite element mesh varied from case to case between 7000 and 15000 elements approximately. This order of magnitude ensured numerically stable results. As shown in Figure 6, a refined mesh was provided in the notched zone where stress concentrations were expected to occur.

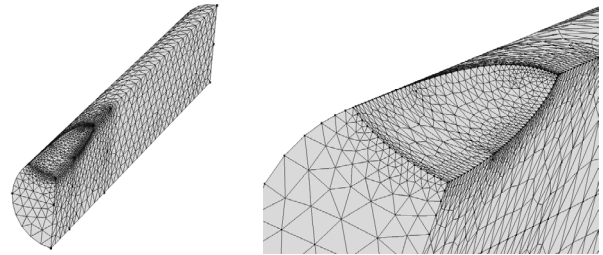


Figure 6: View of the meshed rebar with zoom (right) of the notched zone

3.4 Material properties

The material characteristics laid down in the numerical analysis correspond to a class B500 B steel, according to [13]. The corresponding characteristic bilinear stress-strain diagram, based on [14], is shown in Figure 7 (blue curve). The elastic range of this diagram is defined by a yield strength of $f_{yk} = 500$ N/mm² and Young's modulus $E = 200000$

N/mm². The behavior in the plastic range is characterized by ratio k of tensile strength f_{uk} to yield strength f_{yk} , $k = 1.08$, considering strain hardening, and an ultimate strain of $\varepsilon_{uk} = 5\%$.

In a next step the mean values were estimated from the described characteristic values and the corresponding stress strain relation (Figure 7, red curve) was laid down in the numerical analysis. The mean value of the yield strength was estimated to $f_{ym} = 1.12 \cdot f_{yk} = 560$ N/mm², according to [15]. The slope of the elastic range was kept equal to that of the characteristic diagram, $E = 200000$ N/mm². The same assumption was made for the plastic range. Moreover, the ratio k of f_{um} to f_{ym} was adopted from the characteristic diagram. Hence, the mean values of the tensile strength and the ultimate strain were estimated to be, respectively, $f_{um} = 604.8$ N/mm² and $\varepsilon_{um} = 5.6\%$. It should be noted that the latter is a very conservative value, what should be kept in mind when analyzing the results obtained in the present study.

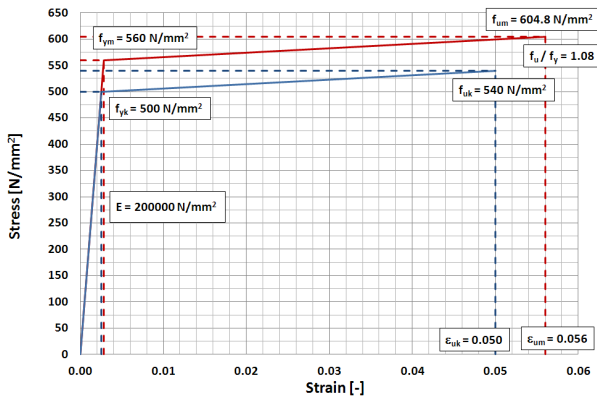


Figure 7: Elasto-plastic material behaviour of steel B500-B. Characteristic curve (blue) and curve adopted in numerical study (red), based on estimated mean values.

In order to account for the multi-axial stress state at the corrosion pits, the von Mises yield criterion in conjunction with an isotropic hardening model has been employed, which is an appropriate and frequently adopted assumption for ductile materials such as steel.

4 RESULTS

4.1 General aspects

In the following, the procedure applied to analyze the obtained results will be outlined. In a first step, the stress-strain diagram for each of the 36 studied cases has been derived. By way of example, Figures 8 and 9 compare results obtained for $d = 12$ mm rebars with, respectively, varying relative pit-depths, p/d (Figure 8) and varying length to depth ratios, a/p (Figure 9). For comparative purpose, in both figures the stress-strain diagram corresponding to the sound bar is as well included. Before those results will be commented in the next section, it has to be stated that the represented stresses σ were determined by ratio of the applied force to the bar, F , and its non-notched cross section, A_{s0} . The strains ε were obtained from equation (3), where ΔL_z is the displacement in axial direction (z -direction, Figure 5) of a particular reference point on the bar, and L_{ref} the distance from this point to the symmetry plane of the notch, which in advance will be referred to as reference length.

$$\varepsilon = \Delta L_z / L_{ref} \quad (3)$$

In accordance with the observations in [1,12], it could be observed that strain determination in bars affected by significant corrosion pits is very sensitive to the choice of L_{ref} , which is attributable to strain concentrations at the pits. Therefore the election of L_{ref} should generally be done with care when testing bars suffering from pitting corrosion. In the present work, deformations have been determined with L_{ref} equal to the recommended minimum gauge length according to ISO 6892:1998 [16]. This has been done in view of an experimental verification of the results, which is currently under progress.

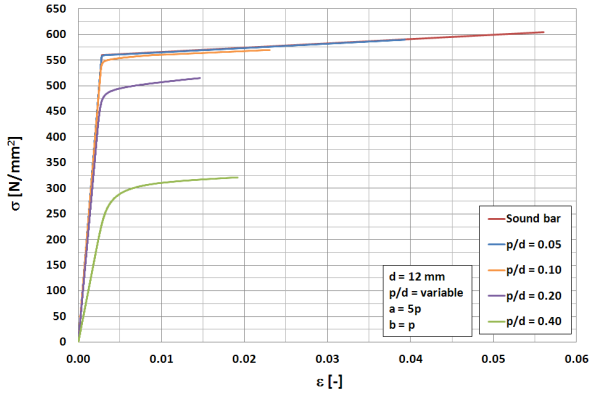


Figure 8: Stress-strain diagrams of bars with $d = 12\text{mm}$, $a/p = \text{const.} = 5$, $b/p = \text{const.} = 1$, and varying relative pit depths, p/d

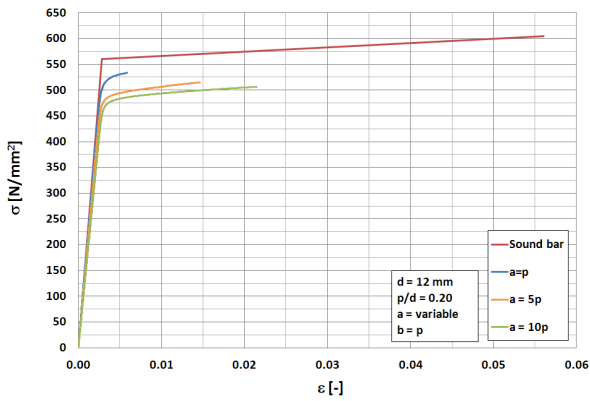


Figure 9: Stress-strain diagrams of bars with $d = 12\text{mm}$, $p/d = \text{const.} = 0.2$, $b/p = \text{const.} = 1$, and varying pit length to depth ratios, a/p

Once the stress-strain diagrams were derived, the principle mechanical properties of the notched bars were obtained: the equivalent stress corresponding to the yield strength of the notched bars, $\sigma_y = F_y / A_{s0}$, defined at the point where strain increment $\Delta\epsilon/\Delta\sigma$ exceeds a defined threshold value of $3.3 \cdot 10^{-5} \text{MPa}^{-1}$, the equivalent stress corresponding to the tensile strength of the bar, $\sigma_u = F_u / A_{s0}$, hardening ratio $k = \sigma_u / \sigma_y$ and ultimate deformation ϵ_u .

Finally, the deduced mechanical properties of the analyzed bars were related to the corresponding values supposed for non-corroded, sound bars and graphically represented as a function of the parameters characterizing the geometry of the pits. This is shown in the following section.

4.2 Cases $d=12\text{ mm}$ and $b/p = 1$

Equivalent stresses

Figure 10 shows that the ratio of equivalent yield stress σ_y to the corresponding value of a sound bar, $\sigma_{y0} = 560 \text{N/mm}^2$, decreases with rising relative maximum pit depth, p/d , circumstance which may be equally observed in Figure 8. In the latter, one may appreciate as well that the same conclusion may be drawn for the equivalent stress to ultimate strength of the bar, σ_u .

From the mentioned figures it may be observed as well that the decrease of σ_y and σ_u , with respect to the corresponding stresses in sound bars, can be judged insignificant ($< 5\%$) for p/d up to 0.1, moderate ($\approx 10\text{-}20\%$) for $p/d = 0.2$ and important ($\approx 45\text{-}55\%$) if ratio p/d attains values of around 0.4. It is also noteworthy that ratios p/d exceeding 0.15 may lead to situations where σ_y falls below the characteristic value of material yield stress, $f_{yk} = 500 \text{N/mm}^2$, represented in Figure 10 by the horizontal dot-dashed line. Moreover, from figures 9 and 10 it may be deduced that slender pits ($a/p = 5$ or 10) entail more pronounced reductions of equivalent stress σ_y , than do short pits ($a/p = 1$).

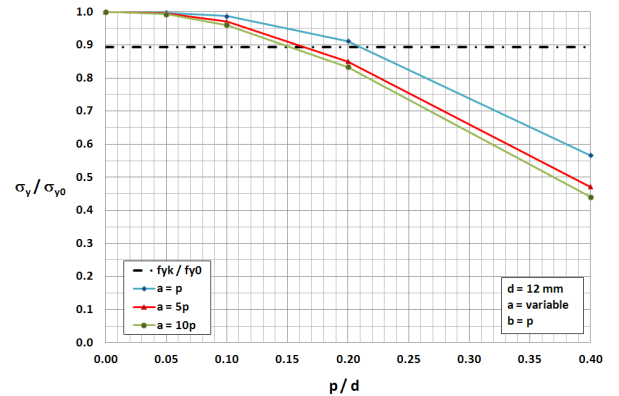


Figure 10: Ratio of equivalent yield stress σ_y of notched bars to corresponding value supposed for sound bars, $\sigma_{y0} = 560 \text{N/mm}^2$, as a function of p/d and a/p ; $d=12\text{ mm}$, $b/p=1$

The observed reduction of load carrying capacity of the bars may be attributed to stress concentrations related to cross section reduction and stress gradient, which is a function of the pit geometry. Stress

concentration at the pit may be observed in Figure 11 for a particular case. Moreover, it must be taken into account that a corrosion pit will change the center of gravity of the bar cross section. Hence an eccentricity is introduced which gives rise to bending moments when the bar is exposed to tensile force. As well known, the combined effect of axial forces and bending moments may reduce cross section resistance of the bar.

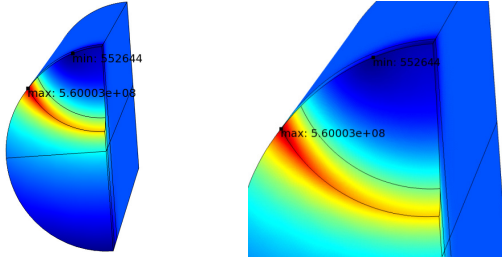


Figure 11: Von Mises stress concentration at corrosion pit, $d = 12$ mm, $p/d = 0.40$, $a/p = 1$, $b/p = 1$

Ductility

As a measure of ductility, the ratio of equivalent ultimate strength to equivalent yield strength, $k = \sigma_u/\sigma_y$, has been computed. Figure 12 shows that variation of k with respect to the here supposed value of non-corroded bars, $k_0 = 1.08$, is insignificant up to relative pit depths of $p/d = 0.2$. Beyond this threshold, even a slight increase of k can be detected. This could lead to the premature conclusion that ductility is not sensitive to pit depth variation. However, from Figure 13, it may be rapidly deduced that such a conclusion would be misleading. As may be observed, the ratio of ultimate strain ε_u of the notched bars to the corresponding value supposed for sound bars, ε_{u0} , generally decreases with increasing p/d , at least until $p/d = 0.2$. Beyond that limit, an increase of $\varepsilon_u/\varepsilon_{u0}$ may be observed which may be attributed to the favorable effect of large, slender pits. Note in that context that an increase of p/d entails by definition an increase of pit length a , and thereby a favorable effect which counteracts the unfavorable influence of maximum pit depth.

It is also interesting to mention that a pit with a small relative penetration depth of 5% ($p/d = 0.05$) causes ε_u to decrease moderately

around 20-30%, when pits are of slender aspect ($a/p = 5$, $a/p = 10$). On the contrary, in case of short pits ($a/p = 1$), the obtained decrease of ε_u is very significant with reductions reaching from 78%, in case of small penetration depths ($p/d = 0.05$), up to 90% for deeper pits.

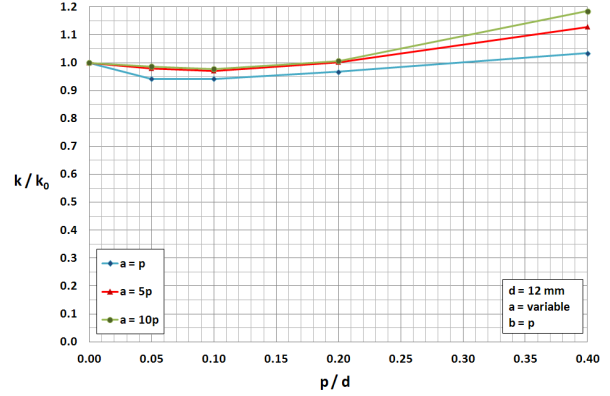


Figure 12: Ratio of parameter $k = \sigma_u/\sigma_y$ to the corresponding value supposed for sound bars, $k_0 = 1.08$, as a function of p/d and a/p ; $d = 12$ mm, $b/p = 1$

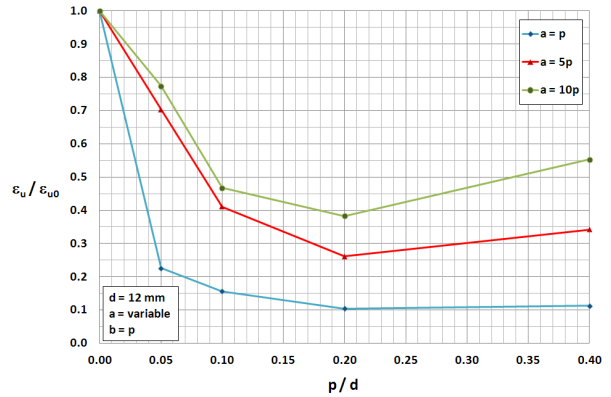


Figure 13: Ratio of ultimate strain ε_u to corresponding value supposed for sound bars, $\varepsilon_{u0} = 5.6\%$, as a function of p/d and a/p ; $d = 12$ mm, $b/p = 1$

The important decrease in ultimate strain, and hence in ductility, can be related to the reduced capacity of the notched bars to undergo significant plastic deformations. While in a sound bar submitted to a tensile force, strain may be supposed to be uniformly distributed over its length (at least until initiation of plastic instabilities upon attaining maximum force), in a locally pitted bar strain concentrations arise at the pits and, in that way, reduce its overall deformation capacity at failure. As exposed before, this has been

observed in some of the reported experimental studies [1,8,9], and could be confirmed by the here presented numerical simulations.

Note also that alarming reductions of ε_u up to 90%, which are obtained when the corrosion pit is short in relation to the bar diameter (Figure 13, case $a/p = 1$), were as well observed in the work from Almussalam [8], as shown in Figure 2. However, in the mentioned study the significant ductility decrease is attributed primary to locally high penetration depths, and the corresponding strain concentrations, on bars suffering in general from very severe corrosion attack. On the contrary, the results presented in Figure 13 show that even a small penetration depth of 5% ($p/d = 0.05$) causes the ultimate strain to decrease about 80%. Intuitively, this seems not realistic and suggests that the results presented in Figure 13 are to some extent conservative, what is probably related to the definition of the material behavior (Figure 7) in the present study. The first results of an experimental study on notched rebars, currently under progress, dedicated to the validation of the here presented numerical results, seem to corroborate this hypothesis.

Moreover, it should be mentioned that the modeling of a single corrosion pit is as well a conservative approach concerning the ductility performance of the rebars since practically the entire plastic deformations will concentrate at this pit.

4.3 Influence of pit width and scale effect

The results presented in the previous section correspond to rebars of diameter $d = 12$ mm and pit-widths characterized by ratio $b/p = 1$ (Figure 4). When incrementing this ratio to $b/p = 2$, an additional reduction of mechanical performance in terms of resistances and ductility is observed, as could be expected. However, this additional reduction is of minor importance, suggesting that pit-width is not as decisive as pit length and depth.

Finally, it is mentioned that scale effect does not alter the mechanical parameters of the notched bars. That could be concluded by comparison of results corresponding to bars of,

respectively, $d = 12$ and 32 mm. For both type of bars, practically identical results are obtained when pit dimensions are kept proportional to the diameter of the bars.

5 CONCLUSIONS

In the present paper the results of a numerical study dedicated to the influence of geometrical characteristics of elliptically shaped corrosion pits on mechanical properties of a B500B type rebar. The most relevant conclusions drawn from the study may be resumed as follows:

The load-carrying capacity of the notched rebars reduces with increasing relative maximum pit depth, p/d . Ratios p/d around 0.2 may entail relatively moderate reductions up to 15%, approximately. The influence of pit slenderness, characterized by ratio of pit length, a , to its depth, p , on load carrying capacity is as well relatively moderate.

Ductility of the notched rebars, expressed in terms of ultimate strain, is very sensitive to variations of pit geometry. Both pit depth and pit slenderness have significant influence on ultimate strain. Slender pits with relative high a/p ratios ($a/p = 5-10$) are in general less harmful than short pits ($a/p = 1$). For the latter, ultimate strain reductions up to approximately 90% were obtained. However, first results of an ongoing experimental study suggest that the here presented numerical results are to some extent conservative what might be related to the definition of material stress-strain relation in the numerical analysis. Further research in that direction is certainly required.

REFERENCES

- [1] Palsson, R., Mirza, M., Mechanical response of corroded reinforcement of abandoned concrete bridge, *ACI Structural Journal*, 99, n° 2, 157-162, 2002
- [2] Apostolopoulos, C., Papadopoulos, M., Pantelakis, S., Tensile behaviour of corroded reinforcing steel bars BSt 500s, *Construction and Building Materials*, 20, 782-789, 2006

- [3] García Alonso, M., Aportaciones al comportamiento resistente de estructuras de hormigón armado afectadas por la corrosión de sus armaduras, *Tesis Doctoral, Universidad Politécnica de Madrid, Escuela Técnica Superior de Arquitectura*, 1995
- [4] García Alonso, M., Alonso Alonso, M^a C., Andrade Perdrix, M^a C., Rodríguez Santiago, J., Influencia de la corrosión en las propiedades mecánicas del acero, *Hormigón y Acero*, n^o. 210, 11-21, 1998
- [5] Du, Y., Clark, L., Chan, A., Residual capacity of corroded reinforcing bars, *Magazine of Concrete Research*, 57, n^o 3, 135-147, 2005
- [6] Moreno Fernández, E., Corrosión de armaduras en estructuras de hormigón: Estudio experimental de la variación de la ductilidad en armaduras corroídas aplicando el criterio de acero equivalente, *Tesis Doctoral, Universidad Carlos III de Madrid*, 2008
- [7] Muñoz Noval A., Comportamiento de vigas hiperestáticas de hormigón armado corroídas y reparadas con mortero. Pérdida de propiedades del acero de refuerzo, y fisuración del recubrimiento de hormigón por corrosión, *Tesis Doctoral, Universidad Politécnica de Madrid*, 2009
- [8] Almussalam, A., Effect of degree of corrosion on the properties of reinforcing steel bars, *Construction and Building Materials*, 15, 361-368, 2001
- [9] Du, Y., Clark, L., Chan, A., Effect of corrosion on ductility of reinforcing bars, *Magazine of Concrete Research*, 57, n^o 7, 407-419, 2005
- [10] CONTECVET, Manual de evaluación de estructuras afectadas por corrosión de las armaduras, *EC Innovation Programme, IN30902I, IETcc-CSIC*, 2001
- [11] Stewart, M.G., Mechanical behaviour of pitting corrosion of flexural and shear reinforcement and its effect on structural reliability of corroding RC beams, *Structural Safety*, n^o. 31, 19-30, 2009
- [12] Cordero, M. 2005, Estudio de la vida útil de estructuras de hormigón pretensado frente a corrosión por cloruros. *Tesis Doctoral, Universidad Politécnica de Cataluña, Departament d'Enginyeria de la Construcció*, Barcelona, 2005
- [13] UNE-ENV 10080, Acero para armaduras de hormigón armado, Acero corrugado soldable B500, Condiciones técnicas de suministro para barras, rollos y mallas electrosoldadas, *AENOR*, Septiembre 1996
- [14] EN 1992-1-1: 2002, Eurocode 2 – Design of concrete structures – Part 1-1: General rules and rules for buildings, European Committee for Standardization, Brussels, December 2004
- [15] Tanner, P., Lara, C., Hingorani, R., Seguridad estructural. Una lucha con incertidumbres, *Hormigón y Acero*, n^o 245, Madrid, 2007, ISSN: 0439-5689
- [16] International Standard, *ISO 6892: 1998 (E), Metallic materials – Tensile testing at ambient temperature*, 1998